

9.5 A Near-Field Modulation Technique Using Antenna Reflector Switching

Aydin Babakhani, David B. Rutledge, Ali Hajimiri

California Institute of Technology, Pasadena, CA

In typical radio transmitters, the signal is modulated at lower frequencies and then up-converted, amplified, and radiated by an antenna. In the absence of multi-path, receivers at different angles observe the same modulated signal, only different in gain factor and time delay. Although a directional antenna radiates more power in some angles than others, the signal transmitted to any direction still carries the same information that, in principle, can be recovered with a sensitive receiver.

This paper presents a near-field reflector switching technique that can generate independently controlled modulated signals for sufficiently different angles of radiation. This technique can be used either to transmit different data in different directions simultaneously, or to generate the correct signal constellation only in the desired direction and scrambled ones for other angles, creating a secure communication link. This approach is also conducive to power-efficient switching PAs, even for wideband non-constant envelope modulation schemes, enabling fast and power-efficient transmitter architectures.

The fundamental principle of this scheme is shown in Fig. 9.5.1, where an antenna (a dipole in this case) is driven by a CW signal of constant amplitude and phase. There is also a reflector (a conductive metal line with comparable dimensions to the wavelength) in close proximity of the antenna that can be shorted or opened at some point along its length using a switch. The reflected signal in a given direction interferes with the main signal radiated by the antenna in that direction. The amplitude and phase of the reflected signal depend on the boundary conditions that the reflector imposes and can be varied by turning the switch on or off. The two states of the switch result in two different phases and amplitudes in the direction of interest producing two distinct points in the I-Q plane. This offers a crude one-bit digital modulation without changing the output power or phase of the PA driving the antenna thus allowing it to operate at its highest efficiency.

Although the single-reflector single-switch configuration of Fig. 9.5.1 provides a basic binary modulation, there is a limited control over where the two modulation points fall. This problem is solved by introducing multiple reflectors each with multiple switches (Fig. 9.5.2a). The experimental results, presented later in this paper, confirm that it is possible to achieve good coverage of the signal constellation using a reasonably large number of reflectors and switches.

Interestingly, a set of switch combinations that generates constellation points of a given modulation in the intended direction will generate *different* constellation points in a different direction, as shown in Fig. 9.5.2b. For a large number of switches and reflectors, there are numerous different switch combinations that can generate almost the same constellation point in a given direction. However, these different switch combinations can be used to generate different points in other directions concurrently or to scramble the signal in the unintended directions to implement a secure communication link by preventing an undesired observer from demodulating the signal.

In this implementation, an on-chip dipole antenna is used with 10 reflectors (5 on each side), each with 9 tuned MOS switches along its length, resulting in a total number of 90 switches and a remarkable 2^{90} ($\sim 10^{27}$) switching combinations (Fig. 9.5.3). The very large number of switching combinations provides numerous ways to generate a desired phase and amplitude (a point on the constellation) in a given direction, creating a large number of addi-

tional degrees of freedom that can be used for concurrency or security. The ability to *simultaneously* send independent information to several directions at the same time using a single transmitter is not achievable using the conventional transmitter architectures.

In practice, making a high-quality switch for use in mm-wave frequencies is challenging. Achieving a small on-impedance requires a relatively large transistor size, which itself limits the maximum achievable off impedance due to its large parasitic capacitance. This problem can be overcome by resonating the transistor parasitic capacitance using a transmission line connected between its drain and its source (Fig. 9.5.3).

The on-chip dipole antenna and the reflectors are implemented using the three bottom metal layers in a 7M 0.13 μ m SiGe BiCMOS process. The antenna, the ten reflectors, the ninety switches, and the digital control circuitry for the switches occupy a die area of roughly 1.5 \times 1.5mm². For additional flexibility, a direct up-conversion coarse control transmitter is incorporated that can be used for quadrant selection. An on-chip VCO generates an up-conversion LO signal.

To minimize substrate modes, the power is radiated from the backside of the chip using a hemispherical dielectric lens [1], as shown in Fig. 9.5.4. In the measurement setup, the radiated power at 61GHz propagates through the air and is received using a horn antenna to generate the received signal constellation. In order to demonstrate the ability to generate arbitrary constellation points, 20 points generated purely by switching the reflectors using 20 different switch combinations are shown on the left hand side of Fig. 9.5.4. It should be noted that the input power and phase of the signal driving the antenna has *not* been changed to achieve the modulation. In addition, on the right side of Fig. 9.5.4, the received signal constellation at a different angle (about 90° off) for *the same* set of switch combinations is plotted. It is evident that these points are completely scrambled, making it practically impossible for a receiver at an undesirable angle to recover this signal, no matter how sensitive it may be. This is in contrast with a traditional transmitter that sends essentially the same modulated signal, albeit with different amplitude scales and phase epochs, in all directions. This measurement demonstrates the feasibility of the idea for security of communication links.

A three-stage fully differential PA (Fig. 9.5.5) is designed to drive the antenna. The base bias voltages of the stages are provided through differential T-line stubs and the output is matched to the next stage (or the antenna for the last stage) using differential T-line stubs. The transmitter has a measured small-signal gain of 34dB, a saturated gain of 25dB, and a saturated output power of at least +7dBm, as shown in Fig. 9.5.6b. The VCO has a phase noise of -100dBc at an offset frequency of 10MHz. Figure 9.5.6a shows a measured received signal constellation in a desired direction covering all quadrants using the reflector switching and coarse tuning for a pre-selected set of points proving the viability of this concept. The complete chip including the on-chip dipole antenna, reflectors, switches, digital control circuits, VCO, transmitter, and test receiver occupies 2.5 \times 5mm², as shown in Fig. 9.5.7.

References:

- [1] A. Babakhani, X. Guan, A. Komijani et al., "A 77-GHz Phased-Array Transceiver With On-Chip Antennas in Silicon: Receiver and Antennas," *IEEE J. Solid-State Circuits*, vol. 41, no. 12, pp. 2795-2806, Dec. 2006.

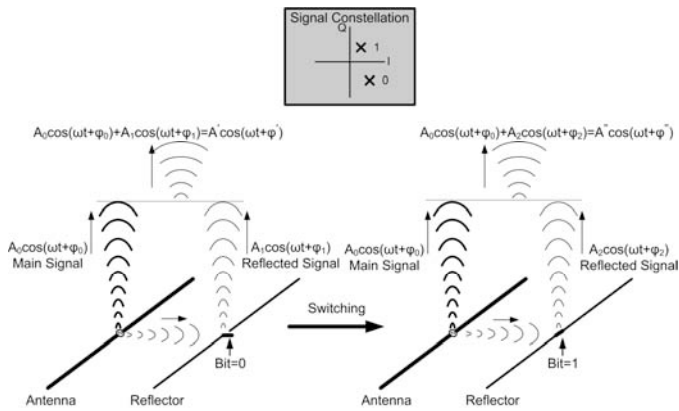


Figure 9.5.1: One-bit signal modulation using a switched reflector.

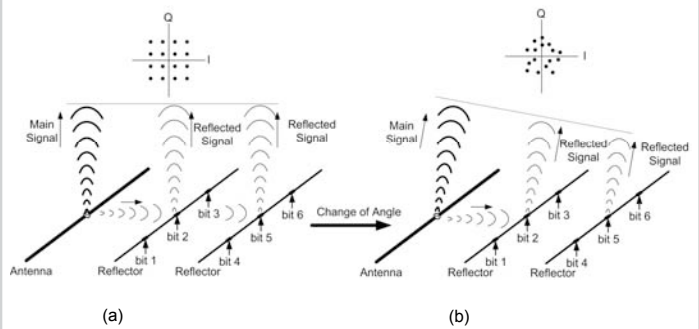


Figure 9.5.2. a) Arbitrary modulation in the desired direction using reflector switching, b) Scrambling of the constellation points with change of direction.

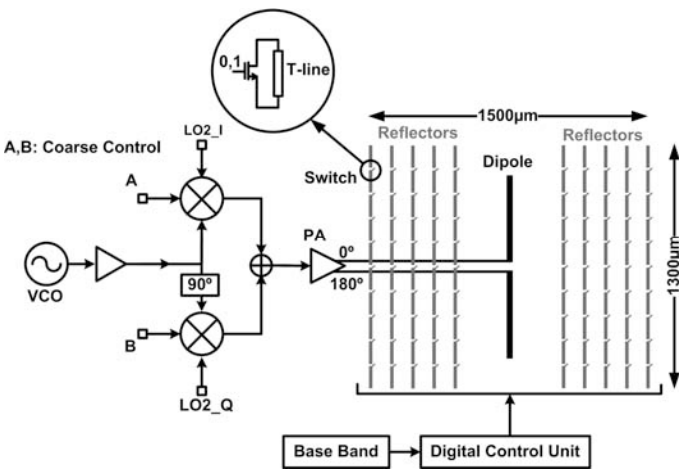


Figure 9.5.3: Near-field reflector switching transmitter.

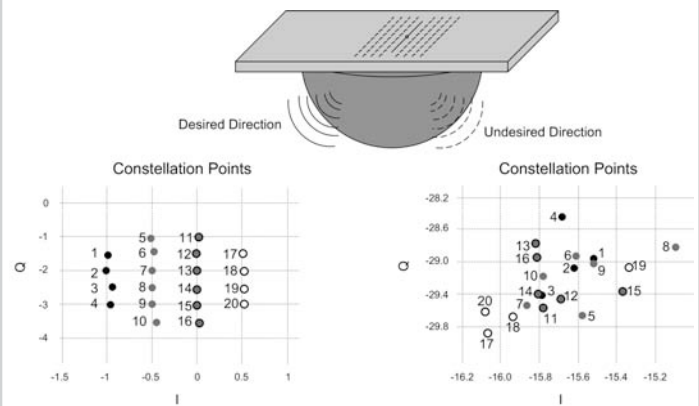


Figure 9.5.4: Measured constellation points at two directions (with switching only).

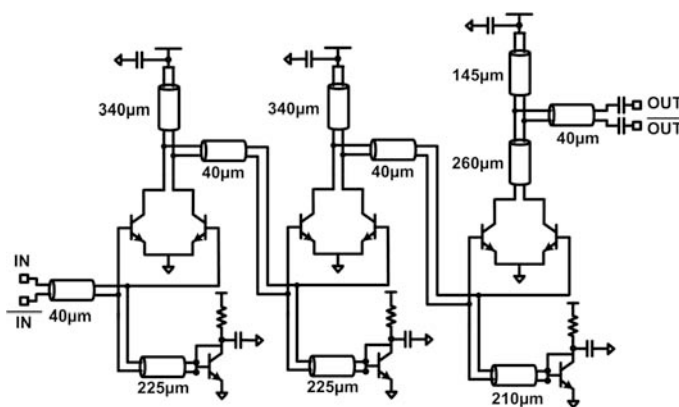


Figure 9.5.5: V-band power amplifier that drives the antenna.

Constellation Points

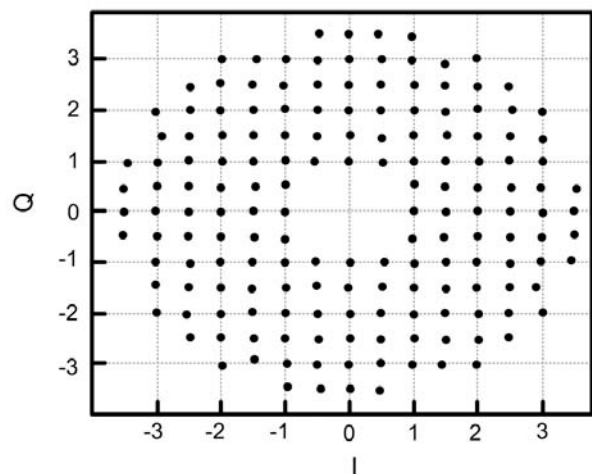


Figure 9.5.6a: Measured constellation points at the desired direction using reflector switching and coarse tuning.

Continued on Page 605

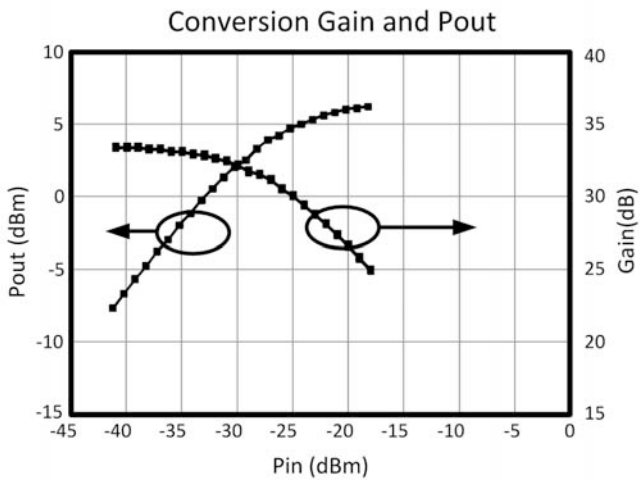


Figure 9.5.6b: Measured transmitter performance.

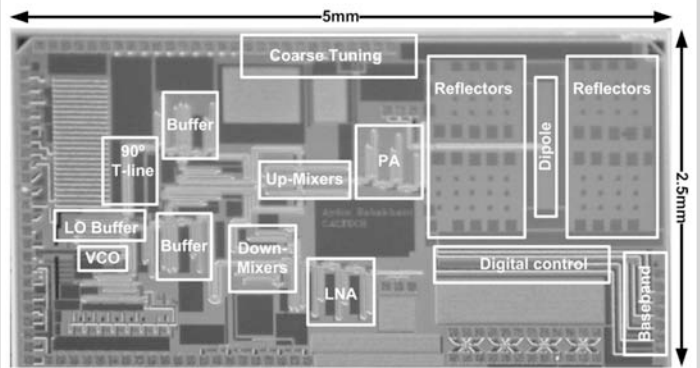


Figure 9.5.7: Chip micrograph.